COMPDYN 2015
5th ECCOMAS Thematic Conference on
Computational Methods in Structural Dynamics and Earthquake Engineering
M. Papadrakakis, V. Papadopoulos, V. Plevris (eds.)
Crete Island, Greece, 25–27 May 2015

RELATIONSHIP BETWEEN THE VARIATION OF SEISMIC CAPACITY AFTER DAMAGING EARTHQUAKES, COLLAPSE PROBABILITY AND REPAIR COSTS: DETAILED EVALUATION FOR A NON-DUCTILE BUILDING

M. Gaetani d'Aragona[1], **M. Polese**[1] **and A. Prota**[1]

[1] Department of Structures for Engineering and Architecture, University of Naples Federico II
via Claudio 21, 80125 Naples, Italy
{marco.gaetanidaragona, maria.polese, andrea.prota}@unina.it

Keywords: Non-ductile, Residual capacity, Performance loss, Repair costs.

Abstract. *Decisions on reparability for damaged buildings after an earthquake are often controversial, and they should properly take into account the variation of building safety level due to damage and the repair costs. A significant indicator for the appropriate course of action is the so-called Performance Loss (PL), that is a measure of seismic safety decay. PL can be determined as a function of the variation of building seismic capacity from the intact to damaged state. This study investigates, by means of a detailed case study, on the expected PL for increasing seismic demand and its relationship with varied building safety level and repair costs. We simulate the response of an existing non-ductile reinforced concrete building using a finite element model that properly accounts for both flexural, shear and axial failure of members and accounts for joints behavior. Different definitions of building collapse are introduced, and Incremental Dynamic Analyses are performed with a representative set of input ground motions both for the intact and damaged structure. In order to evaluate aftershock fragilities, multiple Mainshock-Aftershock sequences are built through suitable scaling of selected accelerograms. Fragility curves for the intact building and the aftershock fragility curves are used to evaluate PL and the variation of collapse probability for main-shocks of increasing return period T_R. Also, corresponding repair costs are determined. The study shows interesting relations between damage levels and repair costs that may be simulated with detailed analyses and associated PL, representing a first insight in the establishment of relations between PL and repair and/or upgrade decisions.*

1 INTRODUCTION

After a seismic event, a number of possible alternatives for dealing with a building damaged by an earthquake, ranging from the acceptance of the damage up to the building replacement are available. For instance, for buildings complying with modern seismic codes, the upgrading is generally not required, but damage must be repaired to bring the building back to pre-earthquake conditions. On the other hand, existing buildings designed with older seismic codes, or gravity load designed ones, are required to be retrofitted or improved as well as repaired, to make the building more robust in future earthquakes. Indeed, while buildings compliant with modern seismic codes, if damaged, only need to restore pre-earthquake capacity, for older buildings a good strategy is to establish damage "triggers" that require not only repair of damage, but also retrofit to improve seismic performance (e.g. [1]).

The most commonly used damage trigger is a threshold value for the loss of strength in the lateral-force-resisting system above which retrofit is required. The Performance Loss index (*PL*) accounts for the loss in lateral strength due to earthquake.

Acknowledging the need for a standard method for calculating the loss levels triggering repair/upgrade requirements, in ATC52-4 [2] a set of retrofit trigger values for selected building typologies was outlined, and more recently, in [2] further specifications on *PL* thresholds and on their calculation based on FEMA 306 [3] were given. However, the suggested *PL* thresholds are based on previous established values of percent loss triggers (e.g. [4]), without a clear quantitative justification for the proposed values. Therefore, there is a clear need to further investigate on criteria and methods for establishing suitable *PL* thresholds governing damage acceptability.

In Polese et al. [5] tools for simplified assessment of *PL* and related repair costs for existing *RC* building classes were presented; the application of those tools within the performance based policy framework introduced in FEMA 308 [6] allowed to show how it is possible to establish *PL* thresholds that are linked to expected repair costs, therefore supporting informed decisions on reparability [7].

However, although it has been shown that simplified methods for the assessment of the behavior of damaged structures yield comparatively acceptable results with respect to detailed methods, e.g. based on nonlinear time history analyses [8, 9], the quantification of these loss thresholds represent a key issue into a reconstruction policy framework, and requires further investigations through detailed cases.

On the other hand, in addition to detailed evaluation of building safety variation, also suitable assessment of expected repair costs should be pursued. Indeed, along with a clear framework for the assessment of lateral loss strength, the estimate of the costs to repair the building to its original state represents a key aspect for the evaluation of building reparability.

Expected repair costs can be determined based on effective damage amount and distribution on the building structural and non-structural system, allowing for accurate assessment towards reparability decisions. In this sense, the *PEER* approach (e.g., [10]) allows the complete assessment of expected damage and costs within a fully probabilistic framework. Different performance assessment can be carried out using *PEER* framework; a recent introduction is the Time-based assessment [11], that evaluate performance over time, considering all possible earthquakes and their probability of occurrence. This loss assessment can be linked to a Time-based assessment of seismic structural safety in order to obtain a full indication of future building's performances.

This paper presents the results of a detailed case study finalized to the assessment of *PL* and repair costs for an existing building when subjected to earthquakes of increasing intensity. Although other studies addressed *AS* fragility assessment with detailed analyses on representative

buildings (see e.g. [12]), or performed detailed evaluation of expected damage and losses for archetype buildings (see e.g. [13]), the present work performs a time-based assessment of both *AS* fragilities and costs, deriving both with reference to selected T_R. Derivation of results in terms of T_R–dependent indices allows to have an easy term of comparison in case of earthquakes having the same return period in the region, without the need to refer to predefined damage states.

In particular, an existing seven-story non-ductile reinforced concrete (*RC*) structure with moment-resisting frame is considered. The response of the building is simulated with a detailed 2D nonlinear multi-degree-of freedom (*MDOF*) model. The model properly account for cumulative damage due to multiple earthquakes through hysteretic rules, damage progress, as well as both shear and axial failure in structural members. In addition, the definition of collapse modes typical for non-ductile frames are considered.

A clear probabilistic framework is introduced for evaluation of building seismic safety decay after a Mainshock (*MS*) associating it to building *PL* and expected repair costs. Multiple damaging earthquake intensities, representative of specific return periods (T_R) for the studied site are considered. Applying Mainshock – Aftershock (*MS*-*AS*) earthquake sequences, *AS* fragilities are built and used to estimate the variation of collapse probability. Also, the repair costs to ideally restore building's intact capacity were estimated and linked to *PL* for analyzed T_R to obtain a full indication of expected building performance and losses.

After definition of significant performance indices (section 2), section 3 synthetically presents the framework and the formulation to build *AS* collapse fragilities conditioned to multiple T_R. Section 4 describes the case study application introducing two different collapse modes that are typical for older *RC* buildings. The collapse fragilities are derived for both intact and T_R-damaged buildings and first results are shown. Section 5 presents the application of the *PEER* framework for the computation of repair costs for the case study. Finally, section 6 presents first considerations about relationship between *PL* and repair costs.

2 BUILDING PERFORMANCE LOSS

The building capacity after an earthquake may be significantly reduced due to the spread of damage all over the building, while the probability of collapse increases. Seismic behavior of damaged buildings, and their relative seismic safety, may be suitably represented by their seismic capacity modified due to damage, the so-called REsidual Capacity *REC* [14, 15].

REC can be defined as a parameter aimed at representing the building seismic capacity (up to collapse) in terms of a spectral quantity. In particular, *REC* of a building is defined as the smallest ground motion spectral acceleration (at elastic period of the Single Degree Of Freedom *SDOF* system equivalent to the real structure) corresponding to collapse state of the building. The performance index *PL* may be determined based on the value of the residual capacity in the intact and damaged states. In particular, considering the collapse capacity in terms of spectral acceleration of the intact building REC_0 and
the variation of *REC* for a structure that is damaged due to an earthquake with a given return period (T_R), *PL* may be expressed as follows:

$$PL = 1 - \frac{REC_{TR}}{REC_0} \tag{1}$$

with REC_{TR} the residual capacity of the *MS*-damaged structure. As shown in [7] this expression of *PL* is equivalent to the expression introduced in [6], where *PL* is derived as a function of the variation of building displacement capacity.

3 TR-DEPENDENT AFTERSHOCK FRAGILITY FRAMEWORK

REC for building damaged by earthquakes of known intensity can been assessed through a dynamic procedure. Fig. 1 illustrates a schematic view of the framework for the dynamic computation of *REC* of damaged building, and the associated *PL*.

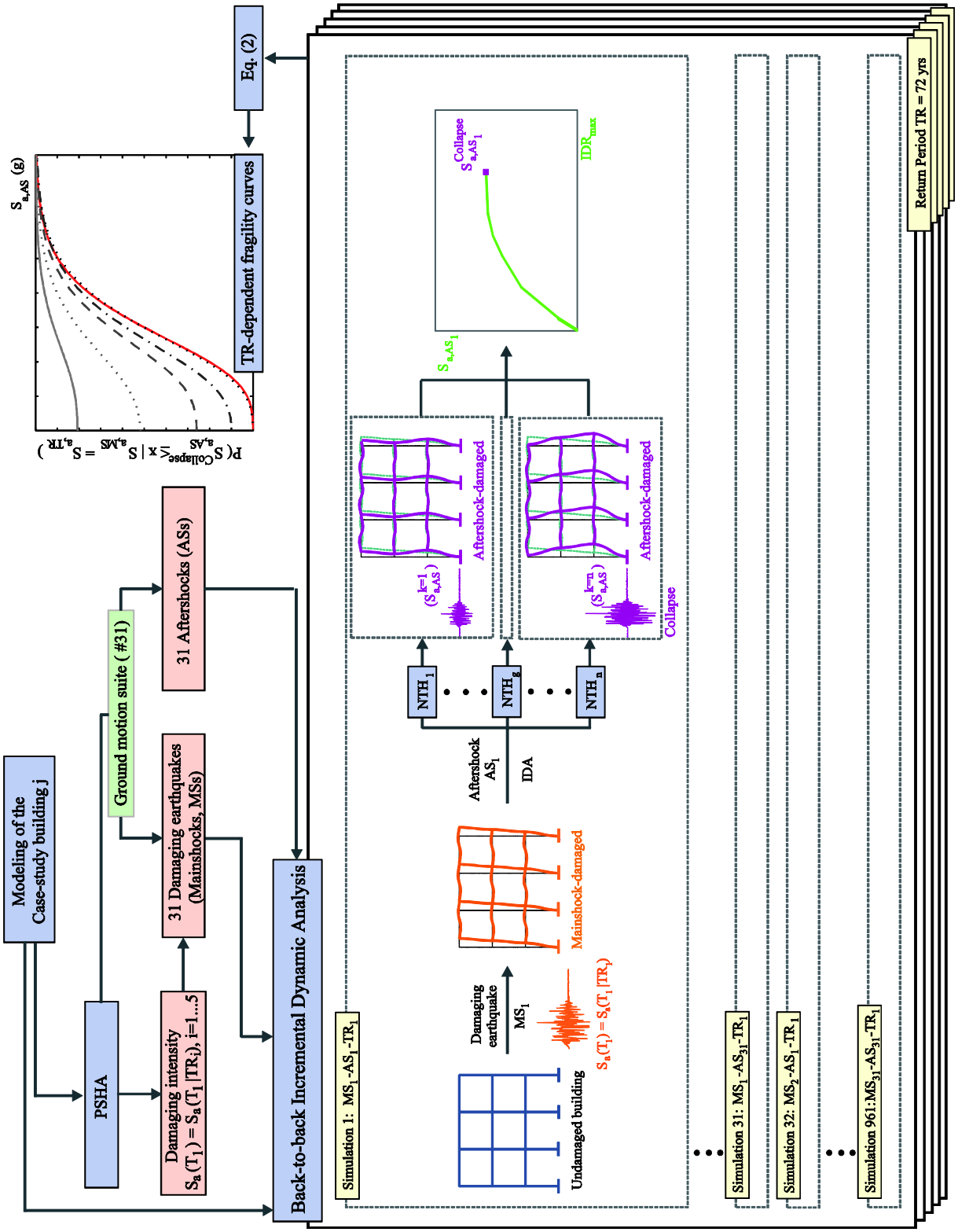

Figure 1: REsidual Capacity assessment framework. Back-to-back *IDA* sequence

The framework is composed of several moduli. After having identified the case-study building, first module entails its elastic and nonlinear structural modeling as well as the assessment of building dynamic properties, such as the fundamental vibration period. This first aspect is addressed for the specific case study in §4.1. Once the properties of the system are calculated, the knowledge of the geographical position of the building and the soil characteristics at the site, allows to perform a Probabilistic Seismic Hazard Analysis (module 2), *PSHA*, the results of which can be used in order to select an appropriate bin of natural ground motions to perform dynamic analyses (§4.2).

Further, *PSHA* allows the computation of earthquake intensities at the site with a given probability of exceedance in a time window (or representative of a given return period T_R). In this study a bin of 31 natural accelerograms was selected to assess the capacity of the intact structure and the REsidual Capacity after damage. With the selected bin of accelerograms, the so called "Back-to-back-*IDA*" (*B2B-IDA*) is used to assess the capacity of building to withstand future earthquakes after damage. Usually, a first earthquake is applied to the undamaged structure in order to reach a specific level of damage; however, in this study the damage level is not known a priori because the sole damaging earthquake intensity is imposed that is representative of a given return period. Once the structure has been damaged, the *IDA* procedure is applied to the damaged structure in order to assess the new capacity of the building. The output of this procedure is an *IDA* curve and an ultimate spectral acceleration capacity of the building for the set Mainshock-Aftershock return period (*MS-AS-*T_R). Note that the accelerograms of the selected bin have been used independently as Mainshock or Aftershock when assessing building's residual capacity.

This simulation must be repeated for each combination *MS-AS* for all considered return periods for a total of 961 simulations for 5 different return periods (4805 simulations) to properly account for record-to-record variability. The result of this framework is a set of fragility curves representing the Residual Capacity of the building conditioned on the return period (i.e., the intensity level of the earthquake conditioned on the site hazard), indicated as "T_R-dependent fragility curves". The simulation of the damaging earthquake and the estimation will be addressed in §4.3, while the mathematical formulation for T_R-dependent fragility curves in §3.1.

In order to evaluate *AS* fragilities, multiple earthquake sequences *MS-AS* are built through suitable scaling of selected accelerograms (see Fig. 2). In particular, the *MS* records are scaled to represent different return periods for the specific area and structure.

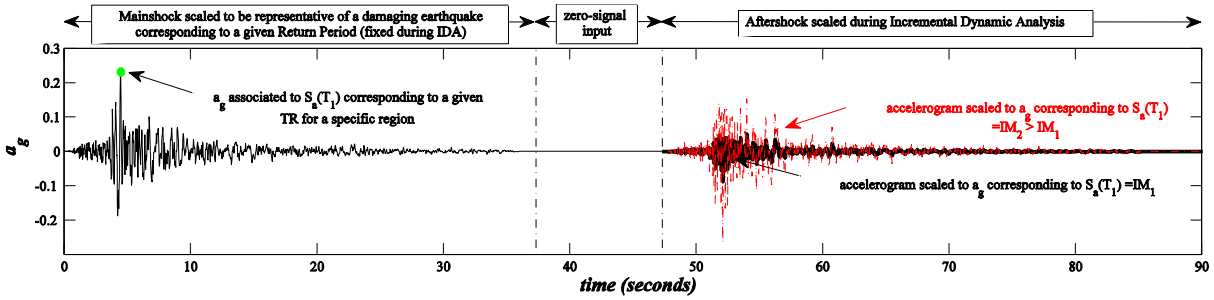

Figure 2: Example of Mainshock-Aftershock sequence.

For the Los Angeles Area and a T_1=1.0 sec, the disaggregation of seismic hazard provides $S_{a,MS}$ values of 0.29, 0.49, 0.65, 0.82 and 1.06g corresponding to the considered T_R = 72, 224, 475, 975, 2475 years respectively (http://geohazards.usgs.gov). For each (scaled) *MS*, nonlinear time history is performed and the response is recorded; then an *AS* record is applied to the *MS*-damaged structure. A time gap of 10 seconds between *MS* and *AS* is considered to allow the

ceasing of vibration produced by the *MS*. Dynamic *AS* analysis is repeated with increasing scale factor applied to the *AS* record, providing *IDA* analysis results for *MS*-damaged structure, until the *MS*-AS sequence causes collapse. To account for the effect of record-to-record variability on structural response *MS*-*AS* sequences are generated using a set of 31 ground motions that are applied as both *MSs* and *ASs*, generating a total of 961 record sequences for each return period.

3.1 Aftershock Fragility Curves Formulation

Starting from the initial damage state produced by a *MS* corresponding to a given T_R, T_R-dependent collapse fragility functions can be built. Because the structure is subject to a series of consecutive events, cumulative damage is accounted for in the estimate of the collapse probability. Considering a seismic sequence consisted of a pair of mainshock *MS* and the consecutive aftershock event *AS*, the aftershock collapse probability conditioned on the *MS* intensity $S_{a,MS}$ can be calculated by considering two mutually exclusive and collectively exhaustive events [16] defined as *C* and *NC*, Eq. (2). *C* accounts for cases where collapse occurs due to the mainshock and *NC* accounts for cases where collapse does not take place due to the mainshock (see [17-19]).

$$P(S^C_{a,AS} \le x \mid S_{a,MS}) = \\ = P(S^C_{a,AS} \le x \mid S_{a,MS}, NC) \cdot P(NC \mid S_{a,MS}) + P(S^C_{a,AS} \le x \mid S_{a,MS}, C) \cdot P(C \mid S_{a,MS}) \tag{2}$$

$$P(S^C_{a,AS} \le x \mid S_{a,MS}, NC) = \int_{\forall \underline{MS}} P(S^C_{a,AS} \le x \mid \underline{MS}, S_{a,MS}, NC) \cdot f(\underline{MS} \mid S_{a,MS}, NC) dMS \approx \\ \approx \frac{1}{N_{NC}} \sum_{i=1}^{N_{NC}} P(S^C_{a,AS} \le x \mid \underline{MS_i}, S_{a,MS}, NC) \tag{3}$$

In Eq. (3) $S_{a,MS}$ is *MS* spectral acceleration corresponding to a specific T_R conditioned on the site hazard, the fundamental vibration period of the intact structure (T_1), and the critical damping ratio assumed; $S_{a,AS}$ is the *AS* spectral intensity at T_1 and $S^C_{a,AS}$ is the *AS* spectral intensity corresponding to collapse. Assuming an equal probability of occurrence for each *MS*, the term $P(NC|S_{a,MS})$ can be estimated as the number of *NC*-cases over the number of *MS* considered (N_{MS}), while $P(C|S_{a,MS})$ can be estimated as the number of *C*-cases over N_{MS} and $P(S^C_{a,AS} \le x|S_{a,MS}, C) = 1$. Hence, the *AS* fragility can be interpreted, for each considered structure and T_R (corresponding to $S_{a,MS}$), as the sum of the mainshock collapse fragility (last term in Eq. (2)), and an inflating term (first term in (3)). $P(S^C_{a,AS} \le x|S_{a,MS}, NC)$ is the collapse probability conditioned on *MS* intensity $S_{a,MS}$ and on *NC* and can be expanded as in Eq. (3). In (4) $\underline{MS}$ stands for the mainshock wave-form vector; $f(\underline{MS}|S_{a,MS}, NC)$ is the joint probability density function for the mainshock wave-form vector given a specific value for $S_{a,AS}$ and given *NC*. The integral in Eq. (3) is an application of the Total Probability Theorem in conditioning on all possible mainshock waveforms conditioned on a given spectral acceleration value. It should be noted that the approximation to the integral in Eq. (3) is based on the assumption that the various mainshock wave-forms have equal probability of occurrence (see [20] for more detail on this kind of approximation).

4 APPLICATION TO A NON-DUCTILE BUILDING

4.1 Description of building's structural model

The building selected for this study is the perimeter moment resisting frame of the Van Nuys Holiday Inn, that is a seven-story eight-bay non-ductile reinforced concrete frame building located in Los Angeles, California, already described in Krawinkler [21].

A two-dimensional finite element *MDOF* model developed using OpenSees [22] is adopted to simulate the seismic response of the building. Beams and columns are modelled using the force-based nonlinear beam–column element [23]. Due to non-ductile details that characterize both of the structures, is expected that the joints may influence the failure mechanism, consequently the joints are modeled using rotational spring elements, the so called "scissor model" by Alath and Kunnath [24], including a pinching hysteric behavior to account for the nonlinear shear deformation of the joint. Similarly, shear and axial failure are expected to occur in non-ductile detailed columns, and consequently shear and axial failure in the columns are modeled using the Limit State material [25]. Bond-slip rotations for beams have been included modifying joint backbone as proposed in [26]. *P-Δ* effects are included. A schematic view of the adopted numerical model is shown in Fig. 3.

The eigenvalue analysis of the intact structure provides a fundamental vibration period of 1.0 sec. A damping of 2% is assigned to the first and third modes using Rayleigh damping. The damping is updated during the first-to-second earthquake analysis at the beginning of each seismic sequence, accounting for the first mode period elongation due to structural damage.

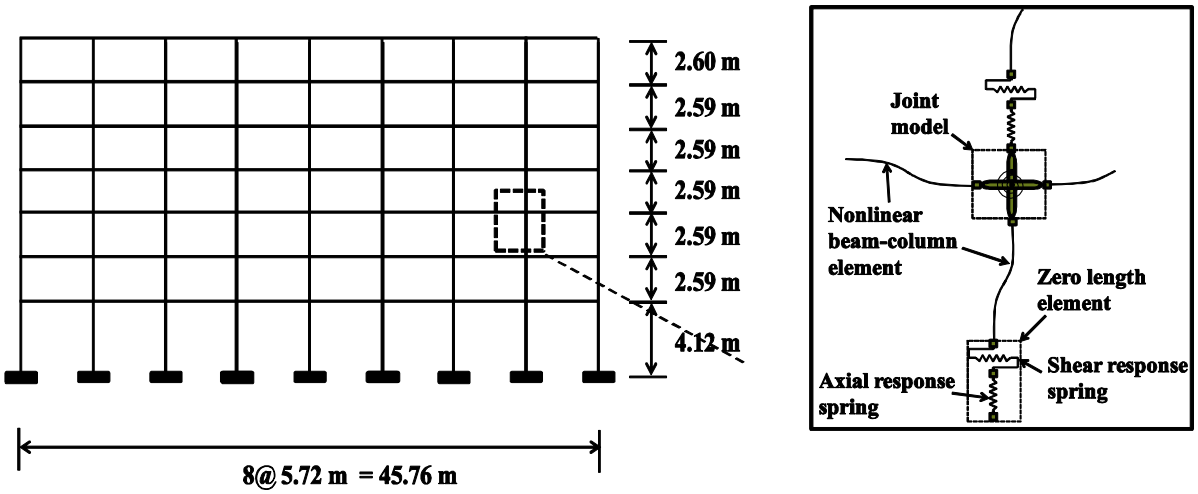

Figure 3: South frame elevation and column, beam and joint models (adapted from Krawinkler, 2005)

4.1.1. Collapse definition

Older RC structures, non-conforming to modern design standards, are likely to experience gravity load collapse prior to side-sway collapse [27]. For this reason, this study considers two possible collapse mechanisms to capture the actual capacity in the model, as firstly proposed in Baradaran Shoraka et al. [28]: Side-sway collapse (*SC*) and Gravity load collapse (*GLC*). The *SC* occurs when a single storey has reached its capacity to withstand lateral loads (i.e., when every column in a given floor has exceeded its residual shear capacity at the same time). *GLC* occurs when vertical load demand exceeds the total vertical load capacity at a given storey. Collapse is detected based on a comparison of storey-level gravity load demands and capacities

(adjusted at each time step to account for member damage and load redistribution). The gravity load demand is considered constant during each analysis.

An internal algorithm monitors the dynamically varying capacity of each element and checks the *GLC* and *SSC* criteria throughout each nonlinear time history analysis to detect the collapse. A bisection algorithm is then implemented to find the collapse capacity with a precision of 0.05g during the *IDA* procedure. The collapse is considered as the first between *GLC* and *SSC*.

4.2 Accelerogram selection

Disaggregation of the seismic hazard for the site is performed based on Bazzurro and Cornell [29]. A shear wave velocity of 218 m/s and a first-mode period of 1 second are assumed. Based on the results of the seismic hazard disaggregation, a set of 31 ground motions is selected from the *PEER* Next Generation Attenuation (NGA) database [30]. To reflect shaking intensity at site, ground motions have been selected using a target $\varepsilon(T_1) = 1.18$ for a reference return period. Ground motions *MS-AS* sequences are generated using this ground motions set where single earthquakes are applied as both *MSs* and *ASs*.

These 31 ground motions have M_w between 6 and 7.6, a closest distance from fault rupture between 7.1 and 48 km and a *PGA* varying between 0.105g and 0.82g. For further information on selection of accelerograms, refer to Baradaran Shoraka et al. [28].

4.3 Fragilities for intact and damaged structure

The fragility computation is based on the use of *IDA* analyses [31], scaled up until collapse is reached; $S_a(T_1)$ is assumed as representative earthquake intensity. To quantify structural response of the intact building, *IDA* is carried out on the nonlinear model of undamaged building using the set of 31 ground motions acting as *MS*. Residual capacity for each *MS* is calculated as the spectral intensity corresponding to the attainment of structural collapse (as defined in previous section); also, median *REC* is determined as the median spectral intensity over all *MSs*, Fig. 4.

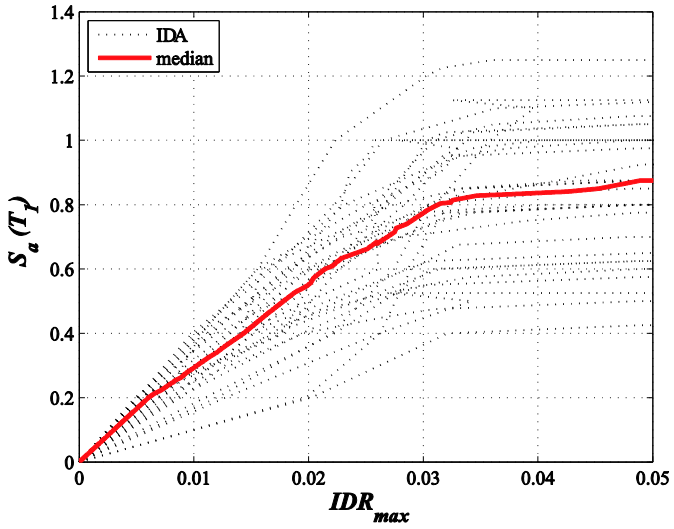

Figure 4: Mainshock incremental dynamic analyses

In order to evaluate *AS* fragilities, multiple earthquake sequences *MS-AS* are built through suitable scaling of selected accelerograms as indicated in §3. In particular, the *MS* record is scaled to represent different return periods for the specific area and structure. The results show

that in the majority of cases a first floor mechanism is activated due to the sole *MS* ground motion; also, usually the Gravity load collapse precede the Sidesway collapse. The type of mechanism usually does not change when considering the *MS-AS* sequence with the same *MS*, this may be attributed to the fact that the damage produced in the building by the *MS*, especially for higher return periods, may significantly affect the future collapse mechanisms that can develop in the building for ASs. *B2B-IDA* is carried out on more than 4800 *MS-AS* sequences (961 *MS-AS* sequence for 5 return periods). The process is computationally intensive, due to the use of a fiber model coupled with the Limit State Material, that allows to account for both shear and axial failure and load redistribution. In order to speed the analyses, OpenSees parallel [22] was used on SCoPE grid at the University of Naples Federico II [32]. Running the analysis on the SCoPE grid in parallel reduces the computation to about 7 days with respect to 240 days required on a desktop computer with 4 processors.

The *REC* of *MS*-damaged building is computed in terms of S_a based on the *IDA* results obtained from *MS-AS* sequences. The results are here represented in terms of fragility curve at collapse. For the undamaged building, the collapse fragility curve is based on the *IDA* results performed on the intact building using the set of 31 ground motions. The collapse fragility curve for damaged building, according to Eq.(2), is calculated based on the *AS* collapse capacities obtained for each of 961 *MS-AS* sequences in which the MS is scaled in order to be representative of the T_R of interest. Fig. 5 illustrates the collapse fragility curves for the intact and damaged building in terms of probability of collapse conditioned on the *MS* for given T_R as a function of *AS* spectral intensity, $S_{a,AS}(T_1)$. The red curve represents the behavior of the intact building.

As the T_R increases, due to the increasing building damage for *MS* application, the collapse fragility curve shift left and up. Because for increasing T_R an increasing number of collapses due to *MS* is detected, the collapse fragility curves for higher T_R have nonzero probability of collapse for $S_{a,AS}$=0.

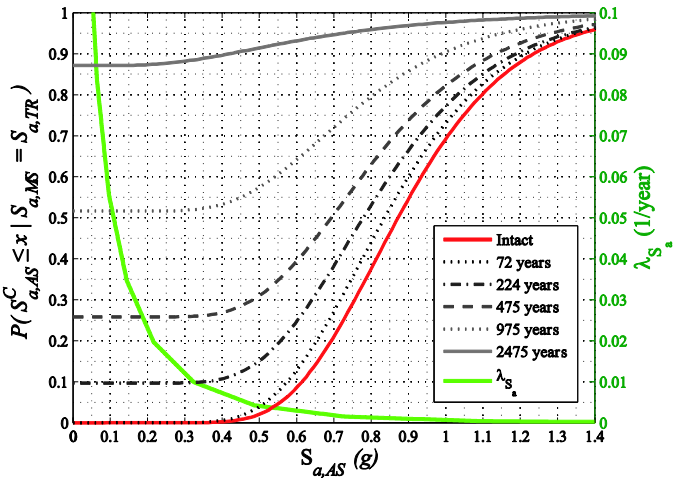

Figure 5: Mainshock TR-dependent aftershock fragility curves and fragility curve for the intact building.

A comprehensive indicator of the structural safety that involves considering both the hazard curve at the site and the collapse fragility curves is the probability of collapse over *t* years. Under the hypothesis that the occurrence of earthquakes in time follows a Poisson process, the probability of one collapse over *t* years can be computed as:

$$P_c(\text{in } t \text{ years}) = 1 - \exp(-\lambda_c t) \tag{4}$$

with λ_c the mean annual frequency of collapse. λ_c can be calculated integrating the collapse fragility curve of the structure over the seismic hazard curve (Fig. 5) at the site using the relation $\lambda_c = \int_0^\infty P(C|im)|d\lambda_{IM}(im)|$ [33], where *P(C|im)* is the probability that the structure will collapse when subjected to an earthquake with ground motion intensity level *im*, and λ_{IM} is the mean annual frequency of exceedance of the ground motion intensity *im*. In order to account for the possibility that the *MS* caused collapse, the Eq.(4) can be rewritten using the Total Probability Theorem by separating *C* and *NC* cases for a given T_R.

The "degraded" REC_{TR}, corresponding to each return period, is computed as the median collapse capacity from the Aftershock *IDA* analyses. Then, the corresponding *PL* is calculated with Eq. (1). Fig. 6 shows the relation between *PL*, *REC*, T_R and the probability of collapse in a time window of 50 years. Note that in more than 50% of cases for $T_R \geq 975$ years collapse occurs due to the *MS*, with a median value of *PL* corresponding to 100% (not shown in figure); obviously, in calculating collapse probability the entire fragility is taken into account, resulting in different (increasing) P_C (in 50 years) for T_R 975 (56%) and 2475 (90%). As expected, for increasing T_R the probability of collapse increases. The same trend is observed for *PL*, while the ratio REC_{TR}/REC_0 decreases.

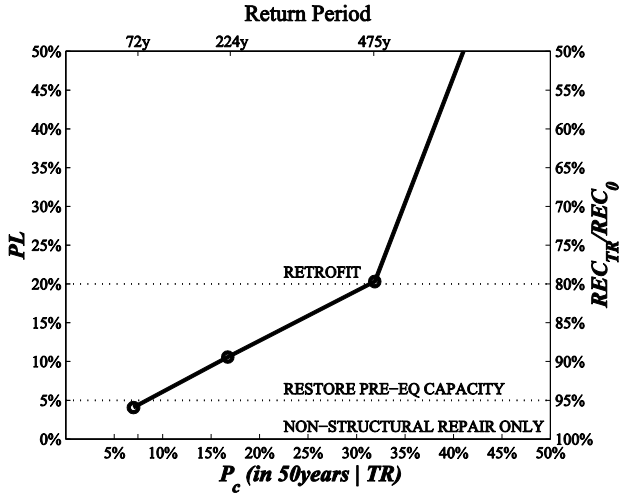

Figure 6: Relations between T_R, P_C in 50 years conditioned to T_R, *PL* and *REC* variation.

The median probability of collapse in 50 years is 6.1% for the intact building while it increases to 7.0% for a 72-years-*MS*-damaged structure and up to a maximum value of 89.6% when considering a return period of 2475 years. In the same figure the restore and retrofit trigger values in terms of *PL*, as suggested in [1] are shown.

Other remarkable observation concern the variation in the fundamental vibration period (T_1), which is strictly related to the global damage [34]. The median variation of the fundamental vibration period with respect to the one for intact building varies with T_R. These values vary in a non-linear way, from a minimum of 0.5% for 72 years return period up to 21% for the 2475 years return period. The same trend is observable for the maximum interstorey drift ratio: the median for T_R=72 years is 0.9% and increases up to 3.7% for T_R=2475 years.

Another interesting parameter is the maximum residual drift, that is often used as limit for technical feasibility of repair intervention and is a directly measurable damage indicator. Its median values vary with T_R from a minimum of 0.02% for T_R=72 years up to 0.46% for T_R=2475 years.

5 ECONOMIC LOSSES

In the previous sections, the collapse performance of a non-ductile *RC* frame was analyzed along with its variation after damaging earthquakes. Here, results are extended to consider economic losses as an additional metric of building seismic performance. In particular, the direct costs associated to repair and/or substitution of the building due to structural and non-structural damage are considered; this metric can support stakeholders' decisions with information, usually in probabilistic terms, about the risk for the building in terms of earthquake economic losses, that is a means of quantifying and communicating risk.

5.1 PEER framework

To evaluate expected economic losses for the studied building, the performance-based framework established by the Pacific Earthquake Engineering Research Center (*PEER*) is adopted [10]. The PEER methodology, briefly summarized in Fig. 7, divides the analysis in 4 subsequent steps, starting from hazard analysis, followed by structural response analysis, evaluation of damage and finally loss analysis; the outcome of each analysis is then integrated using a total probability theorem, allowing to take into account combined numerical integration of all the conditional probabilities and to propagate the uncertainties from one level of analysis to the next, resulting in probabilistic prediction of performance.

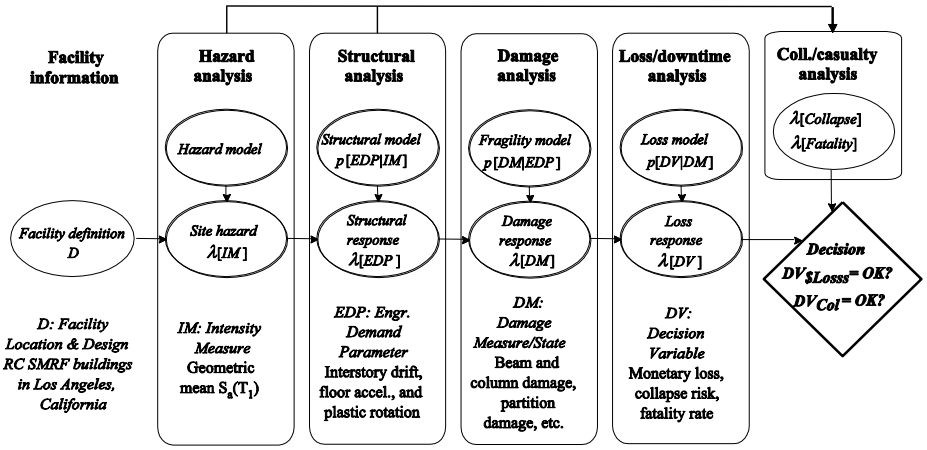

Figure 7: Summary of *PBEE* framework [10]

5.1.1. Hazard Analysis

The first step, the hazard analysis, involves a probabilistic seismic hazard analysis (*PSHA*) [35] to determine the mean annual rate of exceedance of the ground motion of intensity *IM* at the building site. This analysis take into account the earthquake sources, the distance to the fault, local site conditions, etc. The spectral acceleration at the fundamental period is here assumed as *IM*. Using the results of the *PSHA*, a suite of acceleration histories can be selected and scaled to be compatible with the site hazard. This section adopts the same ground motion bin indicated in §4.2.

5.1.2. Response Analysis

The second step involves a suite of nonlinear response history analyses of a structural model of the facility to evaluate its response in terms of engineering demand parameters (*EDPs*), such as peak interstorey drift and peak floor acceleration, conditioned on *IM*. The resulting *EDPs*

will be used as input for the next analysis step to define the damage state reached in each considered component. In this study, the analyses were carried out for the model presented in §4.1, for the five different level of the seismic action corresponding to a 72, 224, 475, 975, 2475 years return period as indicated in §3.1. The response of building is assumed to be the same in two orthogonal directions.

5.1.3. Damage Analysis

The third step, the damage analysis, adopts fragility functions that express the conditional probability that a component (e.g. beam, partition, etc.) reaches or exceeds a particular damage state given the attainment of increasing values of significant *EDPs*. The selected damage states reflect the repair actions needed to restore the component to its undamaged state and corresponding repair costs. Input data for vulnerable components must include information on the types of damage, the structural demands that cause this damage, and the consequences of the damage in terms of repair methods and repairs costs.

Collection of damage fragility functions and unit-repair-cost distribution functions for damageable building components, represent a necessary input to the economic loss analysis. In this study, damage fragilities and repair costs as proposed in [36] were assumed. Ramirez and Miranda [36] provided damage fragility functions for both drift and acceleration-sensitive components, and the expected value of component repair cost expressed as a fraction of component cost as new. It is here noted that lognormal fragility functions are adopted to represent damage distribution, while in this study the uncertainty in repair costs is neglected, adopting expected values as proposed in [36].

Architectural layouts, components and cost of new elements were adopted from Aslani and Miranda [37]; those data are necessary for effective quantification of the amount of damage and costs in the real building. More details can be found in Gaetani d'Aragona [38].

5.1.4. Loss Analysis

The final step of *PBEE* uses the results of previous steps for the computation of the probabilistic losses, which may include repair cost, downtown of activities, and loss of life. In this study, only direct monetary losses (i.e., repair costs) were considered. Further details on the procedure can be found elsewhere (e.g., [11, 39, 40]).

5.2 Evaluation of repair costs

The loss framework outlined in §5.1 was used to carry out the loss simulation for the case-study building. Having simulated the response of the building for different intensities corresponding to return periods ranging from 72 to 2475 years (§3.1), the loss analysis was performed using the fragility data and costs as indicated in §5.1.3. In particular, to solve *PEER* equation integral, a Monte Carlo procedure was adopted. According to Yang et al. [39] and FEMA P-58 [11], the Monte Carlo approach uses inferred statistical distributions of building response obtained from limited suites of analyses to generate additional response parameters (*EDP*) that properly incorporate the effects of modeling uncertainty along with ground motion uncertainty [39]. In this study, 500 realizations were performed for each intensity level. Yang et al. [39] indicated that stable cost estimates can be obtained with as few as 200 realizations. Fragility groups were divided in subsets of group components subjected to the same earthquake demands (i.e., Performance groups, *PG*). For each realization and *PG*, a unique damage state was determined using a uniform random generator over the interval [0,1] considering the probability of the *PG* experiencing each damage state at the *EDP* obtained from structural analysis. Once the damage state for a performance group is identified, the repair action and the associate

repair cost for that performance group is obtained by multiplying cost of new elements by corresponding normalized repair costs by the number of elements in the considered *PG*. If collapse has not occurred, losses are calculated for each realization based on the damage sustained by each component and the consequence functions assigned to each performance group and by summing repair costs of each *PG*. If structural collapse was detected, the total repair cost is calculated using the replacement value of the building plus additional costs related to demolition and debris removal (15% of the replacement value of the building).

Next, direct economic losses are expressed in terms of normalized repair costs (c_r), that are obtained dividing repair costs by the building's replacement value (including expected demolition costs and debris removal as well as cost of new building).

The probability of exceeding a certain level of total normalized repair cost accounting for both the collapse and non-collapse cases can be calculated using the total probability theorem:

$$P(C_r \geq x) = P(C_r \geq x \mid IM, NC)[1 - P(C \mid IM)] + P(C_r \geq x \mid IM, C)P(C \mid IM) \quad (5)$$

where $P(C_r \geq x|IM, NC)$ is the probability conditioned on *IM* when the structure do not collapses that the normalized repair cost exceeds *x*; $P(C_r \geq x|IM, C)$ is the probability of exceeding the normalized repair cost *x* given the collapse, that is actually independent from *IM* and equal to the replacement value of the building; $P(C|IM)$ is the probability of collapse conditioned on *IM*. The complementary cumulative distribution of the total normalized repair costs, is shown in Fig. 8 considering five different hazard levels (i.e. damages due earthquakes characterized by 5 different T_R).

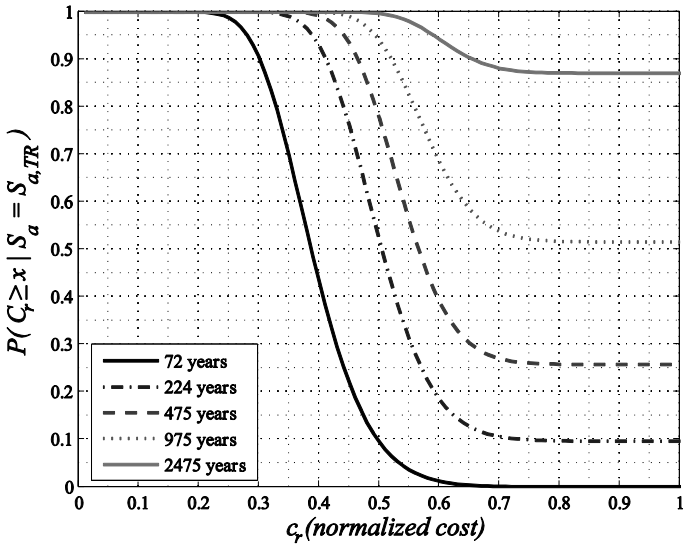

Figure 8: Probability of exceeding normalized cost at five different hazard levels for the American case study.

As it can be seen in Fig. 8, with the increase of the damaging action (i.e., return period) the repair cost inflates making the curve translate rightward. Furthermore, it can be noted that total repair cost of at least 20-25% can be expected even for the lowest considered return period. This high cost is due to the nonstructural components and contents, which significantly contribute to damage and costs even for relatively low levels of seismic action (e.g. for T_R=72 years). It is worth to note that the total normalized repair cost conditioned on the return period of the damaging action at the site is strongly influenced by occurred collapse cases, see second member of the Eq.(5). This effect is particularly evident for higher return periods, for which the curve results translated upward.

6 REPAIR COSTS AND PERFORMANCE LOSS

PL is a measure of variation of building seismic capacity from intact to damaged state and also implicitly account for the seismic safety variation after damage. In addition to performance assessment in terms of safety, repair costs represent a different metric that is normally accounted for in the process of establishing due actions for a damaged building. Hence, it is interesting to observe the relationship between *PL* and repair costs to gather further insights and trend supporting reparability decisions. Fig. 9 shows the median *PL* and the earthquake-induced repair cost c_r determined for the case study building considering increasing return period of the damaging earthquake (the black dots for T_R =72, 224 and 475 years). In order to show the trend for increasing T_R, also dots obtained along the line connecting the *PL*-c_r points of T_R = 475 and T_R = 975 at fixed values of c_r are represented as empty dots.

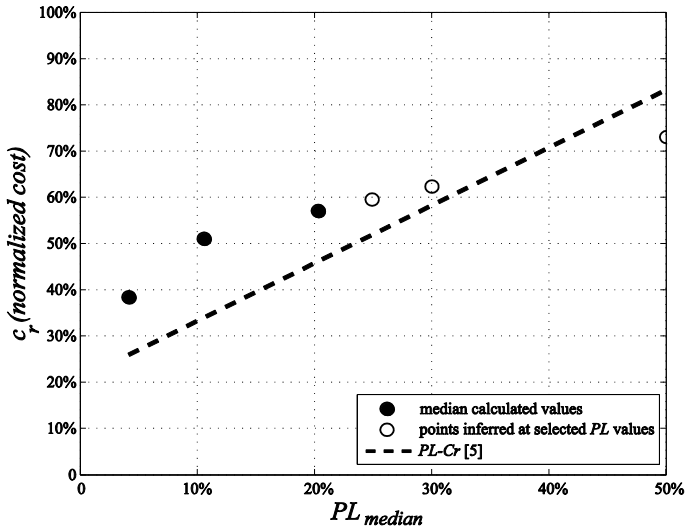

Figure 9: Relation between *PL* and c_r, median values, for the American building and the *PL*-c_r relationship proposed in Polese et al. [5].

In particular, Fig. 9 shows that also for lower *PL* (corresponding to lower return periods) the repair cost is not negligible starting from a median value of about 40%. This effect can be explained considering the source of repair costs, that are structural components, nonstructural components, and building contents. These damageable quantities can be further divided in drift-sensitive and acceleration-sensitive (mainly building contents). The latter quantities result to be severely damaged (contributing to costs) also for lower return periods driving to relatively large repair costs also for a 72 years return period.

The initially increasing trend seems to grow in a less than linear way for higher *PL* (corresponding to higher T_R). This fact suggests some interesting observations. In fact, when the return period increases along with *PL*, then the additional contribution to repair costs is mainly due to drift-sensitive components, whose damage level increases with increasing T_R (and *PL*).

It is interesting to compare *PL*-c_r relationship predicted analytically for this case study, with *PL*-c_r relationship proposed in [5]. This relationship, represented in Fig. 9 with a dotted bold line, was obtained considering a simplified mechanism-based approach that does not account for brittle failures, and observed repair costs after L'Aquila earthquake (2009). In spite of the noticeable simplifications and assumptions for the *PL*-c_r relationship proposed in [5], this first

comparison seems to confirm on the average the proposed trend. Further investigations are required for a better understanding of *PL*-c_r relationship considering different building typologies and hazard level.

7 CONCLUSIONS

The study presented in this paper aims to contribute, with a detailed case study, to the development of tools and applications supporting reparability decisions in a performance based framework. Both the residual capacity variation, that is connected to the variation of safety, and direct economic losses are considered as significant variables for reparability decisions.

In particular, the *PL* index and normalized repair costs were computed with reference to five different return periods, for an existing non-ductile seven-story building in the Los Angeles area.

The response of the building was simulated by means of a detailed 2D nonlinear multi-degree-of freedom (*MDOF*) finite element model. The model properly account for brittle failures and captures typical non-ductile RC frames failure modes.

The analytical model of building was subjected to multiple sequences comprised of two recorded ground motions to simulate the damage produced on the building by main-shocks of a given return period.

The results show that the REsidual Capacity *REC* of a *MS*-damaged building may be significantly smaller (*PL* higher) than the *REC* of an intact building. However, for a *MS* with a T_R=72 years the building capacity is only slightly affected. For increasing T_R, the *PL* increases very fast up to the 100% for *MS* corresponding to T_R= 975 years. For T_R=975 years or larger, the number of collapse cases due to *MS* becomes greater than the non-collapse cases, and the median capacity becomes zero.

Previous studies [12] highlighted that the polarity of the second earthquake may affect the behavior of the building and vary the collapse capacity. However, in this study the effect of polarity on *REC* was neglected and has to be properly taken into account in future works.

Adopting existing component fragilities and repair costs, direct economic losses were computed for the case study building. The results show that repair costs can be significantly high also for low return periods due to the damage of nonstructural components and contents, with a total repair cost of at least 20-25% even for the lowest considered return period. This high cost is due to the nonstructural components and contents, which significantly contribute to damage and costs even for relatively low levels of seismic action.

For increasing T_R the contribution of collapse cases becomes more significant, leading to increasing probability of overcoming the reconstruction costs (c_r=1) already starting from T_R=224 years.

The study performed within this performance-based framework seems to support its applicability for reparability decisions based on quantitative assessment of safety and cost thresholds. Clearly, the level of detail required renders it suitable for specific evaluation of single buildings.

On the other hand, the results can be used to calibrate/verify reparability thresholds to be used in a performance based policy framework of selected building typologies. Indeed, the preliminary comparison with a simplified relationship connecting *PL* and c_r for existing buildings is encouraging towards the possibility to obtain generalized relationships, useful for certain building classes. To this end, further studies are required in order to gather more results on effective thresholds and to assess different factors influencing the trend of variation of repair costs with *PL*, considering different building typologies and hazard levels.

8 ACKNOWLEDGEMENTS

This study was performed in the framework of PE 2014–2016; joint program DPC-Reluis Task 3.3: Reparability limit state and damage cumulated effects and Task 3.5 Methods for the definition of thresholds for seismic retrofit. The S.Co.P.E. computing infrastructure at the University of Naples Federico II was used for parallel computing. The authors would also like to aknowledge Dr. Baradaran Shoraka for sharing OpenSees scripts for the Van Nuys Holiday Inn.

REFERENCES

[1] San Francisco, City of. Post-earthquake repair and Retrofit Requirements, Administrative Bulletins, AB-099, *Department of Building Inspection*, San Francisco, C.A., 2012.

[2] ATC 52–4. Here today—here tomorrow: the road to earthquake resilience in San Francisco, post-earthquake repair and retrofit requirements, applied technology council, prepared for the *Department of Building Inspection (DBI) city and county of San Francisco under the community action plan for seismic safety (CAPSS) project*, 2010.

[3] FEMA 306. Evaluation of Earthquake Damaged Concrete and Masonry Wall Buildings – Basic Procedures Manual. *Federal Emergency Management Agency*, 1998. Washington D.C

[4] CCSF. San Francisco Building Code. *The City and County of San Francisco American Legal Publishing Co*.: Walnut Creek, California, 2010.

[5] Polese M., Di Ludovico M., Marcolini M., Prota A., Manfredi G. Assessing reparability: simple tools for estimation of costs and performance loss of earthquake damaged r.c. buildings, *Earthquake Engineering and Structural Dynamics*, 2014; DOI: 10.1002/eqe.2534.

[6] FEMA 308. Repair of earthquake damaged concrete and masonry wall buildings. *Federal Emergency Management Agency*, Washington D.C., 1998.

[7] Polese M., Marcolini M., Gaetani d'Aragona M., Cosenza E. Reconstruction policies: explicitating the link of decisions thresholds to safety level and costs, *Bull. Earthquake Eng*, submitted, 2015.

[8] Di Ludovico M., Polese M., Gaetani d'Aragona M., Prota A., Manfredi G. A proposal for plastic hinges modification factors for damaged RC columns, *Engineering Structures*, 2013, 51, 99-112, http://dx.doi.org/10.1016/j.engstruct.2013.01.009.

[9] Polese, M., Gaetani d'Aragona, M., Prota, A., Manfredi, G. Seismic behavior of damaged buildings: a comparison of static and dynamic nonlinear approach, paper # 1134, *proceedings of COMPDYN 2013 4th ECCOMAS Thematic Conference on Computational Methods in Structural Dynamics and Earthquake Engineering*, Kos Island, Greece, 12–14 June 2013.

[10] Porter KA. An overview of PEER's performance-based earthquake engineering methodology. *Proceedings of Ninth International Conference on Applications of Statistics and Probability in Civil Engineering*, San Francisco,CA, 2003.

[11] FEMA P-58. Next-generation Seismic Performance Assessment for Buildings, Volume 1 – Methodology, Federal Emergency Management Agency, Washington, D.C., 2012.

[12] Raghunandan, M., Liel, A. B., & Luco, N. Aftershock collapse vulnerability assessment of reinforced concrete frame structures. *Earthquake Engineering & Structural Dynamics*, 2014.

[13] Ramirez, C.M., Liel, A.B., Mitrani-Reiser, J., Haselton, C.B., Spear, A.D., Steiner, J., Deierlein, G.G., Miranda, E. Expected earthquake damage and repair costs in reinforced concrete frame buildings, *Earthquake Engineering Structural Dynamics*; 2012; 41: 1455-1475, DOI: 10.1002/eqe.2216.

[14] Bazzurro, P., Cornell, C. A., Menun, C. A. and Motahari, M. Guidelines for seismic assessment of damaged buildings. *Proceedings of the 13th World Conference on Earthquake Engineering,* 2004. Vancouver B.C., Canada. Paper No. 1708.

[15] Polese, M., Di Ludovico, M., Prota, A., Manfredi, G. Damage-dependent vulnerability curves for existing buildings", *Earthquake Engineering and Structural Dynamics*, 2013; 42 (6), 853-870, DOI: 10.1002/eqe.2249.

[16] Benjamin, J.R. and Cornell, C.A. Probability, statistics and decision for civil engineers, McGraw-Hill, 1970.

[17] Ebrahimian, H., Jalayer, F., Asprone, D., Lombardi, A.M., Marzocchi, W., Prota, A., Manfredi, G. Performance-based Framework for Adaptive Seismic Aftershock Risk Assessment. Earthquake Engineering and Structural Dynamics, Volume 43, Issue 14, pages 2179–2197, November 2014.

[18] Jalayer, F., Asprone, D., Prota, A., Manfredi, G. A decision support system for post-earthquake reliability assessment of structures subjected to after-shocks: an application to L'Aquila earthquake, 2009, *Bull Earthquake Eng*, 2011; 9 (4), pp. 997-1014.

[19] Jalayer F., Asprone D., Prota A., Manfredi G. Multi-Hazard Upgrade Decision-Making for Critical Infrastructure based on Life Cycle Cost Criteria, Earthquake Engng Struct. Dyn, 2011; 40 (10), pp. 1163-1179.

[20] Jalayer, F., Beck, J.L., Zareian, F. Intensity Measures of Ground Shaking Based on Information Theory, *Journal of Engineering Mechanics*, 2012:138 (3), pp. 307-316.

[21] Krawinkler, H. Van Nuys Hotel Building Testbed Report: Exercising Seismic Performance Assessment. P*EER Report 2005/11. College of Engineering*, University of California, Berkeley, 2005.

[22] McKenna, F., Fenves, G. L., Scott, M. H., and Jeremic, B. Open System for Earthquake Engineering Simulation (OpenSees). *Pacific Earthquake Engineering Research Center*, University of California, Berkeley, CA, 2000.

[23] de Souza, R.M. Force-based finite element for large displacement inelastic analysis of frames. *PhD Dissertation*, University of California, Berkeley, USA, California, 2000.

[24] Alath, S., Kunnath, S.K. Modeling inelastic shear deformation in RC beam-column joints. *Engineering Mechanics Proceedings of 10th Conference*, May 21-24, ASCE, Boulder, CO, USA, 1995; 822–825.

[25] Elwood, K. J. Modelling Failures in Existing Reinforced Concrete Columns. *Canadian Journal of Civil Engineering*, 2004: 846-859.

[26] Celik, O.C., and Ellingwood, B.R. Modeling beam-column joints in fragility assessment of gravity load designed reinforced concrete frames. *Journal of Earthquake Engineering*, 2008; *12*(3), 357-381.

[27] Elwood, K.J., Holmes, W.T., Comartin, C.D., Heintz, C., Rojahn, C., Dragovich, J., McCabe, S., Mahoney, M. Collapse Assessment and Mitigation of Nonductile Concrete Buildings: ATC-76-5/ATC-78/ATC-95. *Proceedings of 15th WCEE,* Lisbon, Portugal, 24–28 Sept 2012.

[28] Baradaran Shoraka, M. Collapse assessment of concrete buildings: an application to non-ductile reinforced concrete moment frames. *Ph.D. dissertation*, 2013; Vancouver, BC, Canada.

[29] Bazzurro, P., Cornell, C.A. Disaggregation of seismic hazard. *Bulletin of the Seismological Society of America,* 1999; 89(2): 501–520.

[30] Chiou, B., Darragh, R., Gregor, N., and Silva, W. NGA Project strongmotion database, *Earthquake Spectra*, 2008; Vol. 24, No. 1, pp. 23-44.

[31] Vamvatsikos, D., & Cornell, C. A. Incremental dynamic analysis. *Earthquake Engineering & Structural Dynamics*, 2002; 31(3), 491-514.

[32] Merola L., The S.Co.P.E. Project, *Final workshop of grid projects "PON ricerca 2000-2006, avviso 1575"*, downloadable at http://www.scope.unina.it/datacenter/scopedocs/The_SCoPE_Project.pdf.

[33] Eads, L., Miranda, E., Krawinkler, H., and Lignos, D. G. An efficient method for estimating the collapse risk of structures in seismic regions. *Earthquake Engineering & Structural Dynamics*, 2013; 42(1), 25–41.

[34] Di Pasquale, E., Ju, J. W., Askar, A., & Çakmak, A. S. Relation between global damage indices and local stiffness degradation. *Journal of Structural Engineering*, 1990; 116(5), 1440-1456.

[35] Cornell CA. Engineering seismic risk analysis. Bulletin of the Seismological Society of America 1968; 58(5): 1583.

[36] Ramirez, C.M., & Miranda, E. Building-specific loss estimation methods & tools for simplified performance-based earthquake engineering, *PhD dissertation*, 2009; Stanford University.

[37] Aslani, H., Miranda, E. Probabilistic Earthquake Loss Estimation and Loss Disaggregation in Building. Technical Report No. 157, *John A. Blume Center Earthquake Engineering Center*, Stanford, CA, 2005.

[38] Gaetani d'Aragona, M. Post-Earthquake Assessment of Damaged non-Ductile Buildings: Detailed Evaluation for Rational Reparability Decisions, *Ph.D. Dissertation*, University of Naples Federico II, Italy, 2015.

[39] Yang, T.Y., Moehle, J., Stojadinovic, B., Der Kiureghian, A. Seismic performance evaluation of facilities: Methodology and implementation. *Journal of Structural Engineering,* 2009*;* 135(10): 1146–1154.

[40] Goulet, C.A., Haselton, C.B., Mitrani-Reiser, J., Beck, J.L., Deierlein, G.G., Porter, K.A., Stewart, J.P. Evaluation of the seismic performance of a code-conforming reinforced-concrete frame building - From seismic hazard to collapse safety and economic losses. *Earthquake Engineering and Structural Dynamics,* 2007*;* 36(13): 1973–1997. DOI: 10.1002/eqe.694.